arXiv:1405.4129v1 [cond-mat.mes-hall] 16 May 2014

Fine structure of neutral acceptor states of isolated impurity in zinc-blende semiconductors

M.O. Nestoklon
Ioffe Physical-Technical Institute, Russian Academy of Sciences, St. Petersburg 194021, Russia and CNRS-Laboratoire de Nanophotonique et Nanostructures, 91460 Marcoussis, France

O. Krebs, R. Benchamekh, and P. Voisin
CNRS-Laboratoire de Nanophotonique et Nanostructures, 91460 Marcoussis, France

The properties of neutral acceptor states in zinc-blende semiconductors are re-examined in the frame of extended-basis $sp^3d^5s^*$ tight-binding model. The symmetry discrepancy between envelope function theory and atomistic calculations is explained in terms of over symmetric potential in current $\mathbf{k}\cdot\mathbf{p}$ approaches. Spherical harmonics decomposition of microscopic Local Density Of States (LDOS) allows for the direct analysis of the tight-binding results in terms of envelope function. Lifting of degeneracy by strain and electric field and their effect on LDOS is examined. The fine structure of magnetic impurity caused by exchange interaction of hole with impurity d-shell and its dependence on strain is studied. It is shown that exchange interaction by mixing heavy and light hole makes the ground state more isotropic. The results are important in the context of Scanning Tunneling Microscopy (STM) images of subsurface impurities.

PACS numbers: 75.30.Hx,71.55.Eq,75.30.Et

I. INTRODUCTION

Impurity states in semiconductors have been a major topic for the last 50 years, due to combined fundamental interest and technological importance. In particular, from the theoretical point of view, the related breaking of crystal translational invariance is a tough problem. A prominent milestone is the celebrated article of Luttinger and Kohn[1] where general **k.p**, or Envelope Function Theory (EFT) for electrons and holes in "perturbed crystals" and conditions for decoupling interband and intraband matrix elements of the perturbating potential were discussed. An oversimplified view has emerged that impurity potential can be decomposed into a "gentle" potential having no interband matrix elements, and a "central cell correction" associated to details of the potential near the impurity center. In the seventies, the case of neutral acceptors and the role of valence band degeneracy was thoroughly discussed by Lipari and Baldereschi.[2,3] In short, even in absence of a central cell correction, acceptor states are characterized by a spinor wavefunction with contributions from the heavy, light and possibly split-off valence bands, and just as the host valence band at the zone center, they have a four-fold degeneracy (or three fold degeneracy if spin-orbit interaction is neglected). Generally speaking, EFT approach aims at discarding the local, rapidly varying part of the wavefunction and at establishing an effective hamiltonian acting on supposedly slowly varying envelopes. Perhaps for this reason, in spite of its rigorous formalism, it tends to favor approximations that discard the hardly tractable bond-length scale. For instance, the obvious fact that, due to discrete positions of first neighbors, charge distribution near the impurity center cannot be spherical was essentially ignored, except for a lonely work of Castner[4,5] where the tetrahedral central cell correction $V_{tet}(\mathbf{r})$ is introduced to explain the properties of donors in Si. To our knowledge, the role of $V_{tet}(\mathbf{r})$ for acceptors has not been examined in the literature.

In parallel to these seminal theoretical contributions, a huge number of spectroscopic and transport experiments were dedicated to studies of impurity states in all kind of semiconductors, so that the topic was considered as finished by the end of the seventies. However, there was recently a strong revival of the interest in impurity physics due to the observation of single impurities by scanning tunneling microscopy. The completely unexpected, strongly non-spherical shapes of images associated with acceptors have given rise to passionate debates about their supposed relation to impurity local density of states.[6,7] One of the most intriguing situation was the neutral acceptor state associated with substitutional Mn in GaAs, because in addition to its deep acceptor state character, it carries magnetic properties associated with antiferromagnetic coupling between the "weakly" bound hole and the 5 electrons occupying the $3d$ shell of the Mn atom. It was assumed that the "butterfly" shape of Mn STM images was predominantly due to this magnetic character, until very similar images were obtained in the case of GaP:Cd.[8] Cd in GaP gives a neutral acceptor state with a binding energy in the 100 meV range, close to Mn in GaAs, but obviously has no magnetic interactions. In these two examples, a strong central cell correction is involved, since the binding energy is about 4 times larger than that of a purely coulombic state. The corresponding impurity radius is of the order of a nm, and it was soon realized that atomistic models like tight binding were better suited than **k.p** theory for modeling such impurity states. In particular, many papers have relied on the simple sp^3 model with nearest neighbor interactions because it is supposed to give a fair account

of valence band properties. In this paper, we use the extended basis $sp^3d^5s^*$ model, which is known for giving accurate description of single particle states in semiconductors.

The paper is organized as follow: in section II, we explain the fundamental symmetry mistake of current **k.p** approaches; in section III we compare different tight-binding models, study the difference between shallow and deep acceptors and introduce a spherical harmonic decomposition which gives us a powerful tool for an accurate qualitative and quantitative analysis of results of tight-binding calculations. In section IV, we examine the lifting of acceptor 4-fold degeneracy by strain fields. In section V we examine the lifting of degeneracy by external electric field. In section VI we study the role of exchange interaction and compare two approaches which are used in description of exchange, valid in two limit cases: for single non-interacting impurities and for a semimagnetic alloy. In section VII we briefly discuss the scanning tunneling microscopy images of acceptors. Section VIII concludes the main results. Appendices A and B give some details of calculations.

II. SYMMETRY MISTAKE IN CURRENT ENVELOPE FUNCTION THEORIES

For decades, the main tool for qualitative description of semiconductor micro- and nanostructures was the **k.p** theory. However, there are many examples that without special care the **k.p** approximation fails to reproduce some basic properties even qualitatively. A large set of such failures are connected with oversymmetrizing the problem considered. Examples are heavy-light hole mixing at the interfaces,[9,10] $\Gamma - X$ mixing,[11,12], valley[13–16] and spin[17,18] splitting induced by the interfaces, etc.

The same problem arises when one wants to describe properties of a substitutional impurity in the **k.p** framework.[19] Naive approach using Luttinger Hamiltonian[1] together with Coulomb potential and a short-range potential representing[20,21] the central-cell correction (accounting for chemistry of the impurity) fails to reproduce some qualitative properties, due to the incorrect symmetry of the problem.[4,5] Indeed, Luttinger Hamiltonian has the O_h point symmetry[2] and the Coulomb potential has full rotational $O(3)$ symmetry. However, for a substitutional impurity this potential is not centered at the inversion center of O_h in diamond lattice, but at an atomic site of the zinc-blende (or diamond) lattice, that only has the T_d point symmetry. Therefore, independently of Cation/Anion inversion asymmetry, the substitutional impurity problem has intrinsic T_d symmetry (which excludes inversion center), and accurate treatment of the impurity must take into account this reduced symmetry. For a purely Coulomb potential, symmetry reduction would appear due to tetrahedral (octupolar) charge distribution on nearest neighbors,[4,5] while for an iso-electronic center it would be linked to symmetry of impurity chemical bonding. However, both in O_h symmetry and T_d symmetry the ground level of the hole has Γ_8 symmetry and four-fold degeneracy. Symmetry reduction changes the spacial structure of the wavefunctions, but it is not reflected by additional energy splitting of the levels. This explains why the symmetry mistake in current **k.p** theories (that was actually mentioned in Ref. [2]) has not been revealed long ago in experimental investigations. Finally, it is worth noting that the deeper the impurity level is, the larger quantitative effect of symmetry reduction will be. Obviously, the merit of atomistic approaches (like atomistic pseudo-potentials or tight-binding) in this context is that they automatically include correct symmetries.

III. TIGHT-BINDING CALCULATIONS

Here we focus on tight-binding (TB) calculations of neutral acceptor states (or valence-type iso-electronic centers) and first explain the importance of using an extended-basis tight binding model. It is often believed that the simple sp^3 TB model gives a fair account of semiconductor valence band, while more complex schemes like the $sp^3d^5s^*$ TB model become necessary only when details of the conduction band zone edge valleys come into play. However, it has been proved that the restricted-basis sp^3 nearest neighbor TB model cannot account quantitatively for the valence-band dispersion of III-V semiconductors,[22] in contrast to the $sp^3d^5s^*$ model.[23,24] Precisely, for GaAs the Chadi sp^3 parameters give Luttinger parameters $\gamma_1 = 5.37$, $\gamma_2 = 0.90$, $\gamma_3 = 1.81$, which are rather far from the $sp^3d^5s^*$ values $\gamma_1 = 7.51$, $\gamma_2 = 2.18$, $\gamma_3 = 3.16$, the latter being in excellent agreement with experimental results. These differences mean erroneous effective masses and an underestimate of valence band warping in the sp^3 model. In fact, there are large differences for valence band dispersion throughout the Brillouin zone. It follows that the kinetic energy part of the impurity hamiltonian (about 100 meV for the deep neutral acceptor GaAs:Mn) is not correctly calculated in the sp^3 model. The difference may be estimated separately for effective Bohr radius $a_0 = \hbar^2\varepsilon_0\gamma_1/e^2m_0$ (33% difference), strength of the spherical spin-orbit interaction estimated from dimensionless coefficient[2] $\mu = (6\gamma_3+4\gamma_2)/5\gamma_1$ (31% difference) and cubic contribution[2] $\delta = (\gamma_3-\gamma_2)/\gamma_1$, which is 26% different in two models.

Also, it is worth to mention that without the empty d-orbitals, it is impossible to account quantitatively for the strain dependence of band structure even in bulk semiconductors.[24–27]

A. Shallow and deep acceptors

The properties of the acceptor states in **k.p** approach are usually obtained by adding to the Coulomb potential the central cell correction which may be used in different

forms,[20,21] but generally it is some short-range potential which accounts for chemical properties of the impurity atom. In the tight-binding approximation central cell correction naturally comes as (i) a valence band offset of the virtual material which contains impurity atom (for instance Mn cation) and a counterpart (e.g. As anion) and (ii) change of band structure of the host material due to strain field near impurity. Strictly speaking, there is no freedom in choice of the tight-binding parameters as parameters of this virtual "impurity" material (which is actually a metal) should be also fitted to *ab initio* and/or experimental data. However, for the sake of simplicity and taking into consideration that the states are not particularly sensitive to most of the tight-binding parameters of a single atom, we model "general" acceptor by modifying tight-binding parameters of the matrix adding only artificial valence band offset. It is worth to note that accurate tight-binding treatment with modification of tight-binding parameters[6] implies change of parameters not only of the impurity atom, but also of the nearest neighbors, and two-center hopping integrals connecting them. Since the main effect of this procedure is the renormalization of diagonal energies, in the following we adopt a simplified approach of adding a potential similar to that used in Ref. 28:

$$U(r) = \frac{e^2}{\varepsilon r} + U_{cc} \exp\left(-\frac{r^2}{a_{cc}^2}\right). \qquad (1)$$

This approach allows us to study how hole state localized at the acceptor behaves by changing very few parameters of central cell correction and neglecting details of the chemical structure of impurity. In the following we will use a fixed central cell correction radius $a_{cc} = 2.5$Å.

We consider GaAs as a prototype semiconductor, and unless opposite specification, acceptor states associated with substitution of a group II element on a cation site. The binding energy (E_b) as a function of central cell correction is presented in Fig. 1. One may see that the dependence of E_b on central cell correction potential is highly non-linear. The change of binding energy due to central cell correction is proportional both to central cell correction U_{cc} and amplitude of the wavefunction at the impurity. Increasing U_{cc} we increase both, so the dependence of the binding energy on U_{cc} is non-linear.

The calculation here is made using a rather large (262 144 atoms which form a cube with edge $\sim$ 18 nm) supercell, in order to minimize the width of the "impurity miniband" formed due to the periodization of the problem. For the purely coulombic case, we have in the $\Gamma - X$ direction a residual bandwidth less than 0.9 meV, to be compared with the 26.88 meV average binding energy. This large supercell allows the calculation of acceptor excited states (which crudely may be labelled "2S" and "2P") also displayed in Fig. 1. The widths of these excited state minibands remain quite small (approximately 2.15 meV for first two excited levels), because they are confined by topological minigaps, and their calculated binding energies are reasonable. Yet, it is clear that the excited eigenstates are not as reliable as the ground state. Finally, the quantitative results of Fig. 1 depend on the whole set of material tight-binding parameters, in particular those defining the relative weights of anion and cation contributions in valence band Bloch functions. For more ionic materials, the weight of anions is stronger and the relative importance of central cell correction on first neighbors in comparison with substitutional cation site is increased.

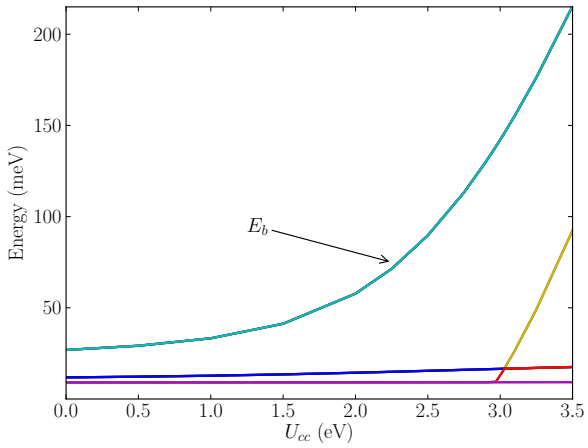

FIG. 1. Binding energy for a neutral acceptor state in GaAs as a function of central cell correction. One may note strongly non-linear behavior. For small central cell correction, binding energy due to Coulomb potential remains almost unchanged, but starting from some value it starts to increase rapidly. Above $U_{cc} = 3$ eV a new level associated with the split-off band shows up.

The wavefunction of the acceptor hole state for the case of shallow ($U_{cc} = 0$ eV, $E_b = 26.88$ meV), intermediate ($U_{cc} = 2.5$ eV, $E_b = 89.7$ meV), and deep ($U_{cc} = 3.5$ eV, $E_b = 215.4$ meV) acceptors are shown in Fig. 2 to illustrate how sensitive the shape of the wavefunction to the binding energy. Even for shallow acceptor, there is pronounced difference between 001 and 110 directions which stems from the valence band warping. It is well seen that upon increasing binding energy, initially close to spherical state starts to feel the microscopic structure of the zinc blende lattice and becomes more and more "tetrahedral".

B. Spherical harmonic decomposition

While extremely helpful from a qualitative point of view, the type of visualization used in Fig. 2 does not provide a quantitative tool for wavefunction analysis, which is of utmost importance when one gets interested in trend effects of perturbations or change in parameters.

Note that through the rest of the manuscript, we will sometimes use term "wavefunction shape" instead of Local Density Of State (LDOS). To avoid confusion, it is

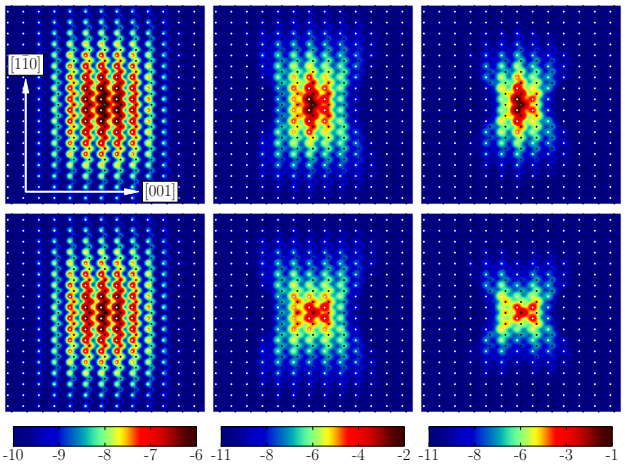

FIG. 2. (110) plane cross sections of the impurity state LDOS (log scale) for some characteristic cases: from left to right, Coulombic center with binding energy $E_b = 26.88$ meV, acceptor with $E_b = 89.70$ meV, and $E_b = 215.4$ meV. Note different color scales. States still have fourfold degeneracy. Atoms are indicated with black (Ga) and white (As) dots. Upper raw for the wavefunction in impurity plane, lower for 4-th atomic plane above.

worth to mention that actual spinor wavefunctions are never plotted because most of the figures correspond to degenerate levels for which the choice of wavefunctions inside Hamiltonian eigensubspace is not unique.

To allow for the desired quantitative analysis, we performed the fit of tight-binding wavefunctions obtained in calculations with **k.p**-like wavefunction as a 3D decomposition in spherical harmonics.

To perform successful fit, we first smooth tight-binding amplitudes by dressing them with gaussians.

$$n^{TB}(\mathbf{r}) = \sum_{\alpha} |C_{i\alpha}|^2 \frac{e^{-(\mathbf{r}-\mathbf{r}_i)^2/a^2}}{(\sqrt{\pi}a)^3} \qquad (2)$$

where $C_{i\alpha}$ are the tight-binding coefficients at i-th atom and $a \simeq 1.73$ Å is chosen to be of the order of interatomic distance and $\mathbf{r}_i$ is the position of i-th atom.

Then we fit the smoothed amplitude (2) with a function

$$n(\mathbf{r}) = \sum_{l,m} f_{lm}(r) Y_{lm}(\Theta, \phi) \qquad (3)$$

using the freely available software archive SHTOOLS (shtools.ipgp.fr). Since we are interested in the description of LDOS amplitudes, that are real, here we use real harmonics rather than complex spherical harmonics. The real harmonics are defined in Appendix A.

The set of functions $f_{lm}(r)$ allows a quantitative description of the shape of the tight-binding LDOS of the impurity ground state. More precisely, noting that $\int r^2 f_{00}(r)$ is the probability to find electron in the region limited by the radius of integration, we propose to use the functions $r^2 f_{lm}(r)$ to estimate how "important" harmonics $Y_{lm}(\Theta, \varphi)$ is in the impurity wavefunction. Also, the r^2 factor helps revealing aspherical features that characterize the "shape" of impurity LDOS at some distance from impurity center. An example may be found in Fig. 3, where spherical harmonics decomposition of the level with binding energy $E_b = 89.7$ meV from Fig. 2 is shown.

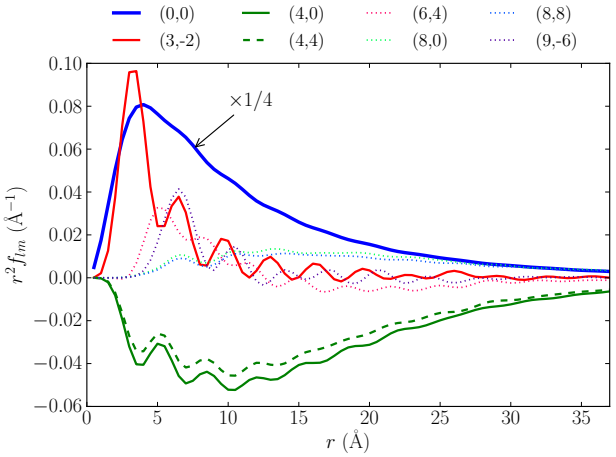

FIG. 3. Functions $r^2 f_{lm}(r)$ for some harmonics. One may see that dominating contributions come from 0-th and 4-th harmonics. The dominant contribution $r^2 f_{00}(r)$ is scaled with a factor 1/4. Significant amount of 3-rd harmonics may be attributed to tetrahedral arrangement of the first neighbours of the impurity.

As one might expect, dominant contribution for 1S-like hole level is for $l, m = 0, 0$ harmonics. Luttinger Hamiltonian through the warping term[3] proportional to $\gamma_3 - \gamma_2$ introduces harmonics $l = 4, m = 0, \pm 4$. Tetrahedral site potential[4,5] adds the harmonic $l = 3, m = -2$. Above mentioned contributions together may combine and introduce higher harmonics. Later we will discuss the effect of strain which reduces the symmetry and introduces additional terms in the harmonic decomposition (3). In such case, the main additional contribution has the same symmetry as the applied perturbation, see below.

Note the oscillatory behaviour of these functions in Fig. 3: they correspond to atomic texture of the crystal. For a few first coordinate spheres the atoms are distributed at some fixed distances with gaps between them which produces these oscillations. Gaussians in (2) tend to smooth them out, but there is a compromise between smoothing atomic texture and showing variations of harmonics in space. To further simplify the "shape description", the set of $r^2 f_{lm}(r)$ functions can be replaced by a set of numbers P_{lm} representing the integrals over some range of r, that we shall use for a rough estimation of LDOS anisotropy:

$$P_{lm} = \int_{r_1}^{r_2} r^2 f_{lm}(r) \qquad (4)$$

where in the following we choose $r_1 = 6$ Å and $r_2 = 30$ Å to concentrate on a region without few neighboring atoms where validity of spherical harmonics decomposition is questionable and one better use atomistic results directly. For example, in the case of Fig. 3, we have $P_{00} = 2.42$, $P_{40} = -0.804$, $P_{44} = -0.69$ and $P_{80} = 0.238$.

It is worth to note that cubic anisotropy has a maximum for binding energy around 100 meV. For a Coulomb center, the kinetic energy is small and spherically symmetric contribution dominates. Increasing central cell correction and binding energy, we increase importance of cubic contribution P_{40} and P_{44}, up to the moment when wavefunction becomes strongly localized and higher harmonics prevail, see Fig. 4.

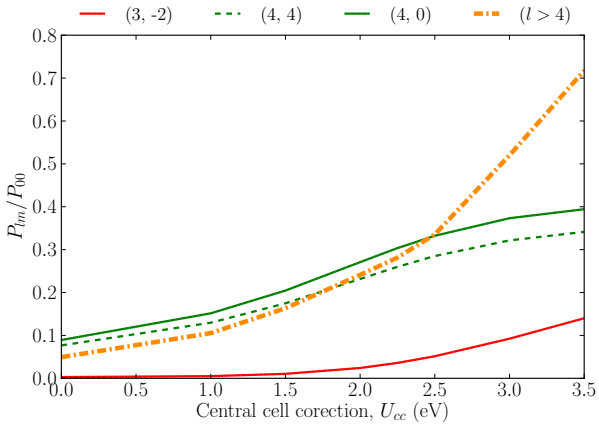

FIG. 4. Absolute value of normalized coefficients $|P_{lm}/P_{00}|$ as a function of central cell correction. Harmonics with $l > 4$ are summed. It can be seen that 4-th harmonics which originates from terms with cubic symmetry in Luttinger Hamiltonian dominates and rises with the binding energy, until wavefunction becomes "too localized" and higher harmonics start to dominate.

IV. EFFECT OF STRAIN, ANALYSIS OF IMPURITY STATE

As long as the impurity potential respects T_d symmetry, the hole ground state of the hole retains Γ_8 symmetry and remains four-fold degenerate, just as in the classical, oversymmetric **k.p** approach. Time-inversion symmetry for a half-integer spin means that in absence of magnetic field and exchange interaction levels remain two-times degenerate. As a result, a perturbation respecting time-inversion symmetry (like strain, quantum confinement, electric field...) can only lead to splitting of one fourfold degenerate level into two Kramers-degenerate doublets. In this section, we use the spherical harmonics decomposition method and examine how different uniaxial strains change the ground state LDOS.

The effect of strain is included into tight-binding following a generalized approach of Ref. 25 similar to one given in Ref. 26: the transfer matrix elements are scaled based on bond-length change and diagonal energy shift and splitting are introduced, based on a local strain tensor. This approach is shown to give a quantitatively correct description of strain in $sp^3d^5s^*$ tight-binding approximation.[25,27]

A. Strain along [001]

When strain along [001] is applied, symmetry of the lattice is reduced from T_d to D_{2d} and four times degenerate level with symmetry Γ_8 is split in two levels $\Gamma_6 \oplus \Gamma_7$ in accordance with compatibility table of the representations of this group.[29] Spherical harmonics decomposition shows how strongly the shape of hole density changes when the strain is applied.

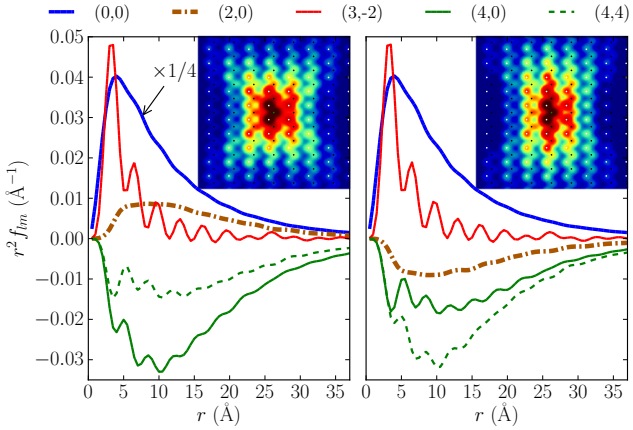

FIG. 5. Comparison of dominant functions $r^2 f_{lm}(r)$ for the two levels obtained after ground state splitting by a weak [001] strain. Strain value is 0.1%, and central cell correction is 2.5 eV. Left panel shows level with binding energy 88.58 meV and right panel shows level with binding energy 91.08 meV. For the left figure $P_{20}/P_{00} = 0.109$ and for the right one $P_{20}/P_{00} = -0.115$. Note that summing of the amplitudes for the two doublets, one gets almost the same amplitudes as for the unstrained, fourfold-degenerate case. Binding energies are arbitrarily counted from the top of unstrained GaAs valence band.

The change in the P_{lm} values is quite pronounced. It is pretty obvious that the four-times degenerate ground state which looks more or less like cube is split by the strain to two levels: one is elongated along strain and the other is flattened in that direction. These changes are reflected in the additional P_{20} and in the related changes in P_{40} and P_{44}

The figures show that the spherical harmonics decomposition gives an adequate numerical criterion to study this change of the shape.

B. Strain along [110] and [111]

Even though the symmetry is lower in the case of both [110] and [111] strain directions in comparison with [001] strain, without magnetic field we cannot split fourfold degenerate level more than in two Kramers doublets and the energy dependence on the strain applied is rather poor. The spherical harmonics decomposition however allows carefully examine how exactly the shape of the two levels changes. From Fig. 6 one may see that again second harmonics of the significant value and opposite sign appears for the two levels.

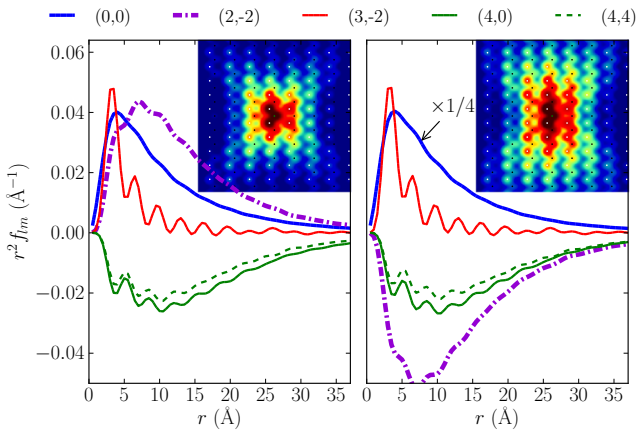

FIG. 6. The same as in Fig. 5, but strain along [110]. Left panel shows level with binding energy 84.77 meV and right panel shows level with binding energy 95.52 meV. For the left figure $P_{2-2}/P_{00} = 0.431$ and for the right one $P_{2-2}/P_{00} = -0.526$.

Similar results may be obtained for the strain along [111].

Obviously, the splitting of neutral acceptors states by uniaxial strain reflects the corresponding splitting of valence band edges. For instance, the larger splitting for [110] than for [001] strain is linked with the larger value of the deformation potential $d \sim -5$ eV coming into play in the former case compared to $b \sim -2$ eV governing the latter. However, it is important to note that bound state splitting is significantly smaller than band-edge splitting[30–32] (twice smaller in given example), because "heavy" and "light" holes remain admixed in the split states.

V. EFFECT OF EXTERNAL ELECTRIC FIELD

Another interesting case of symmetry-breaking perturbation is the effect of an electrostatic potential. External electric field is known to cause a quadratic Stark shift of hydrogenic impurity ground state, but at the same time it reduces the point group symmetry of the acceptor problem. For instance, electric field along a [001] axis reduces the symmetry from T_d to C_{2v}, which implies an admixture of $(3/2, 3/2)$ and $(3/2, -1/2)$ components in the spinorial wavefunction. Calculation shows that in addition to the quadratic Stark shift a linear splitting occurs. For a binding energy of 100 meV, the wave-function polarizability is weak, and both the linear splitting and quadratic shift have a similar value (0.3 and 0.25 meV respectively) for $F = 100$ kV/cm. From the symmetry considerations, we expect qualitative differences when changing the electric field orientation with respect to cubic symmetry axis. Details will be published elsewhere.

Decomposition in spherical harmonics shows expected appearance of dipole momentum which is associated with coefficient $(l = 1, m = 0)$ and reflects the symmetry of the perturbation. This dipole component P_{10}/P_{00} of a sum over four levels is linear with electric field (about 5% for 100 kV/cm) while the dipole momentum for the split levels is enhanced (decreased) to about 3%.

VI. THE CASE OF MAGNETIC ACCEPTOR

So far we considered the effect of perturbations that break the T_d symmetry and lift the fourfold degeneracy of the neutral acceptor state. In this section, we consider the more subtle situation of the perturbation by exchange interaction with d-electrons, like in the emblematic case of GaAs:Mn. By itself, Heisenberg coupling between bound hole and the d-shell electrons does not reduce the symmetry, but it increases the size of the Hilbert space and mixes angular momenta of the components into total angular momentum of the system. The related many-body interaction completely changes the impurity spectrum by introducing a spin dependent fine structure. Here, we compare the fine structures obtained using either the isotropic (Heisenberg) or axial (Ising) exchange couplings, and calculate how they are influenced by a (001) strain. A striking result is that isotropic exchange makes ground state LDOS more resistant against the strain-induced symmetry breaking.

In the following we will extensively use the notation 3/2 and 5/2 while for the exchange interaction we adopt spherically symmetric approximation. Two microscopic sources of reduced symmetry may be considered: crystal field splitting of the states of half-filled Mn d-shell and anisotropic exchange. Both are allowed by T_d symmetry and may split excited states. However, existing experimental measurements[33] show that these splittings are extremely small compared with spherically symmetric part and we neglect them completely.

A number of available experimental data[34–38] shows that the ground state of hole localized at Mn acceptor is three times degenerate. Adopting isotropic model, it is interpreted as hole state with angular momentum 3/2 interacting with Mn d-shell with angular momentum 5/2 which gives four states with total angular momenta $\mathscr{F} = 1, 2, 3, 4$.

It is well established that exchange interaction in single {Mn + hole} complex is relatively small. Some authors estimate the value ε which is a half splitting between ground and first excited level to be of the order of 5 meV,[39–41] some report even smaller values about 1-2 meV.[42–44] There are also papers[28] about the determination of the parameter $N_0\beta$ used to describe p-d exchange in GaMnAs materials, but the link to the 2-spin exchange (ϵ) depends on the wavefunction of the acceptor state on the A^- core. In the model of Bhattacharjee (see below) the typical value for $N_0\beta$ would agree with epsilon about 5 meV. In the following we will consider a value 5meV. This allows us, following Bhattacharjee[28], to start from calculations of the ground state of hole bound to acceptor neglecting exchange interaction (but of course with account on spin-orbit splitting) and then add exchange interaction. This scheme is valid due to the fact that the binding energy $E_b \simeq 100$ meV is significantly larger than exchange interaction splitting $\varepsilon \simeq 5$ meV. Schematic view of the levels structure is given in Fig. 7.

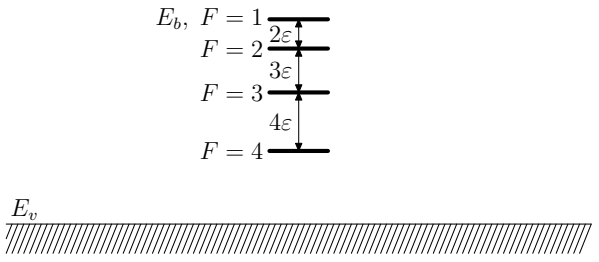

FIG. 7. Scheme of the Mn impurity levels. In the isotropic approximation the ground level of single impurity has total angular momentum $F = 1$.

Wavefunction of this composite system may be obtained using standard procedure:[45]

$$|F,m\rangle = \sum_{|m_1|\le\frac{3}{2}} C^{Fm}_{\frac{5}{2}m-m_1,\frac{3}{2}m_1} \left|\frac{5}{2}, m-m_1\right\rangle \left|\frac{3}{2}, m_1\right\rangle, \tag{5}$$

where $C^{Fm}_{Jm_2,Sm_1}$ are Clebsh-Gordan coefficients. We will not use (5) explicitly because numerically it is easier to obtain the same result as a diagonalization of exchange Hamiltonian operator matrix.

The Hamiltonian of the problem reads as

$$\mathcal{H} = \mathcal{H}_0 + \mathcal{H}_{ex} \tag{6}$$

where $\mathcal{H}_0$ is the kinetic energy plus impurity potential and $\mathcal{H}_{ex}$ is the exchange interaction. We first solve the problem with $\mathcal{H}_0$ exactly in the tight-binding approximation and afterwards diagonalize full Hamiltonian of the system $\mathcal{H}$ in the truncated basis of four function which form the ground state. This follows the general scheme proposed in Ref. 28, the discussion of validity of this approximation will be given later.

Without strain, the solution of $\mathcal{H}_0$ is the four times degenerate hole level which is in terms of $\mathbf{k}\cdot\mathbf{p}$ approximation $1S_{3/2}$ hole level.[46]

$$\mathcal{H}_0 \left|1S_{3/2}, i\right\rangle = E_b \left|1S_{3/2}, i\right\rangle \quad i = 1,2,3,4 \tag{7}$$

Including strain, this four times degenerate level splits in two. Due to time-inversion symmetry, the remaining two-times degeneracy holds for arbitrary strain. Applying magnetic field one may in principle fully split the ground state in four levels. In the following we do not rely on exact ground state degeneracy.

$$\mathcal{H}_0 \left|1S_{3/2}, i\right\rangle = E_i \left|1S_{3/2}, i\right\rangle \tag{8}$$

Following Bhattacharjee[28] we add the exchange interaction in the simplest form

$$\mathcal{H}_{ex} = -\mathscr{J}(\mathbf{r})\mathbf{J}\cdot\mathbf{S}, \tag{9}$$

where $\mathbf{S}$ is the spin operator acting in Mn spin configuration space and $\mathbf{J}$ is the spin operator acting on hole wavefunction.

Then we consider exchange interaction in the truncated basis which is obtained as a Cartesian product of the ground state of the hole (8) and spin states of Mn.

$$H^{ex}_{li,kj} = \left\langle \frac{5}{2}, l \right| \left\langle 1S_{3/2}, i\right| \mathcal{H}_{ex} \left|\frac{5}{2}, k\right\rangle \left|1S_{3/2}, j\right\rangle. \tag{10}$$

Hole wavefuncion in the tight-binding approach is a sum over atoms

$$\left|1S_{3/2}, j\right\rangle = \sum_{n\alpha} c^j_{n\alpha} \left|\mathbf{r}_n, \alpha\right\rangle. \tag{11}$$

In the $sp^3d^5s^*$ model α runs through 20 basis orbitals.[24]

As long as exchange interaction is local, it is natural to assume that $\mathscr{J}(\mathbf{r})$ is nonzero at Mn atom only. Under this assumption (10) reduces to

$$H^{ex}_{li,kj} = -\mathscr{J}(0) \sum_{\alpha\beta} c^{i*}_{0\alpha} c^j_{0\beta} \left\langle \frac{5}{2}, l \right| \langle r_0, \alpha| \mathbf{J}\cdot\mathbf{S} \left|\frac{5}{2}, k\right\rangle |r_0, \beta\rangle, \tag{12}$$

where we start enumeration from Mn. This equation reduces to

$$H^{ex}_{li,kj} = -\mathscr{J}(0) \sum_{\gamma=1..3} \{S^{5/2}_\gamma\}_{lk} \sum_{\alpha\beta} c^{i*}_{0\alpha} \{J_\gamma\}_{\alpha\beta} c^j_{0\beta}. \tag{13}$$

Here $S^{5/2}_\gamma$ are standard spin matrices of the total momentum 5/2 and J_γ are matrices of the spin operator in the tight-binding basis

$$\mathbf{J}_{\alpha\beta} = \langle r_0, \alpha| \mathbf{J} |r_0, \beta\rangle. \tag{14}$$

To write explicit form of the matrix (10) we need to compute matrix elements of the spin operator. Detailed derivation of it is out of the scope of current paper, we comment this procedure briefly in appendix B.

The wavefunctions with account on exchange are then found as a solution of eigenproblem

$$\sum_{kj} \left[E_i\delta_{ij}\delta_{lk} + H^{ex}_{li,kj}\right] \xi^{\mathscr{F}}_{kj} = \epsilon_{\mathscr{F}} \xi^{\mathscr{F}}_{li}, \tag{15}$$

where $\mathscr{F}$ enumerates both total spin of the state F and its projection m. Energies of the levels are $\epsilon_{\mathscr{F}}$ and the wavefunctions are

$$|\mathscr{F}\rangle = \sum_{ij} \xi_{ij}^{\mathscr{F}} \left|1S_{3/2}, i\right\rangle \left|\frac{5}{2}, j\right\rangle . \tag{16}$$

Or, explicitly in the tight-binding basis,

$$|\mathscr{F}\rangle = \sum_{n\alpha} \left(\sum_{ij} \xi_{ij}^{\mathscr{F}} c_{n\alpha}^{i} \left|\frac{5}{2}, j\right\rangle \right), |\mathbf{r}_n, \alpha\rangle \tag{17}$$

from which one may easily compute tight-binding amplitude of the hole wavefunction

$$n(\mathbf{r}) = \langle \mathscr{F}|\mathscr{F}\rangle = \sum_{n\alpha} \left(\sum_{ijl} \xi_{ij}^{\mathscr{F}*} \xi_{lj}^{\mathscr{F}} c_{n\alpha}^{i*} c_{n\alpha}^{l} \right) \langle \mathbf{r}_n\alpha|\mathbf{r}_n\alpha\rangle . \tag{18}$$

Note that the scheme used here is valid also in a small magnetic field or in extreme case of very dilute alloy. However, when the splitting due to external or effective magnetic field is larger than exchange interaction of single Mn+hole complex ($\simeq$ 5 meV), classical spin description[47,48] should be used instead.

In Fig. 8 we present a structure of levels the hole ground state localized at Mn impurity neglecting exchange interaction completely (left panel); by using the scheme (6-18) (central panel); and considering Ising exchange with fixed classical vector $\mathbf{S} = (0, 0, S)$ (right panel) as a function of strain applied along [001].

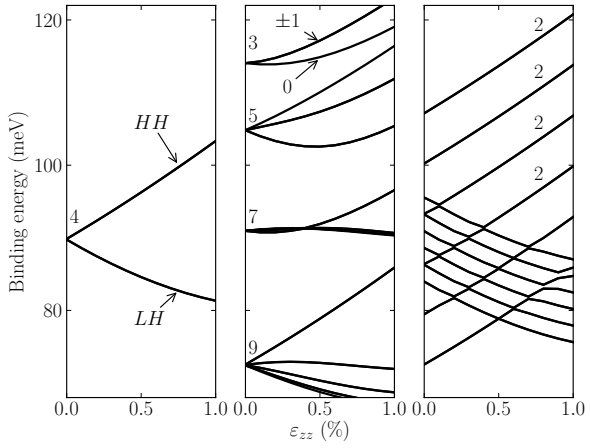

FIG. 8. Splitting of the Γ_8 hole ground state without (left panel) and with (center panel) account on exchange interaction with Mn d-shell. Strain along [001] axis. For comparison, we also show results if we coinsider exchange operator as $\mathcal{H}_{ex}^{I} = J_z \otimes S_z$ Energy zero corresponds to top of valence band in unstrained GaAs.

It is clearly seen that in semi classical Ising description which acts as a local magnetic field, the splitting added to each level is proportional to the product of Mn spin projection and hole spin projection. The distance between levels is independent on strain along [001] because such strain only adds additional splitting between $\pm\frac{3}{2}$ and $\pm\frac{1}{2}$ states of the hole. All levels are two times degenerate because in this approach $E_{+s+j} = E_{-s-j}$ and $E_{-s+j} = E_{+s-j}$ (here s and j are respectively Mn and hole spin projections).

In contrast, scheme (6-18) gives four levels which are three, five, seven and nine times degenerate in accordance with quantum mechanical angular momentum summation. Which is more important, this splitting is lifted by applying the strain to the structure because the states with different angular momentum projection have different heavy/light hole ratio and feel their splitting by strain.

To analyze the interplay between exchange interaction and strain in more details, in Fig. 9 we show the ratio P_{20}/P_{00} as a function of strain applied along [001] direction calculated with and without account on exchange interaction. This ratio quantitatively shows the oblateness of the corresponding states.

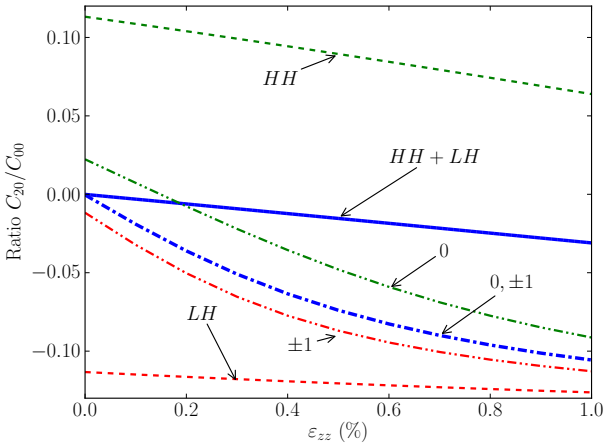

FIG. 9. Ratio P_{20}/P_{00} as a function of strain applied along [001]. Solid line shows this ratio for a sum over four states which originate from Γ_8 ground state. Dash lines show this ratio for two dublets in which ground state is split under strain. Dashed-dot and dash-dot-dot lines show anisotropy for the lowest in energy levels with account on exchange interaction with impurity with angular momentum 5/2. Dash-dot line shows it for the sum of three levels with total angular momentum 1 and two dash-dot-dot lines show it for the levels which may be associated with total angular momentum projection 0 and ±1.

From Fig. 9 it is clear that without exchange interaction spherically symmetric four-times degenerate level is split by the strain in two levels with opposite oblateness which may be attributed to heavy and light hole. Exchange interaction by mixing heavy and light hole into three states with total angular momentum 1 makes the ground state significantly more isotropic. Which is im-

portant, the resulting levels shape is almost linear with the strain.

We would like also to comment the validity of the approximation (6-18) for the description of the exchange interaction. Eigenproblem with the Hamiltonian (6) may be solved exactly in the tight-binding framework, but this assumes the solution in product space which is rather expensive from the computational point of view. Effective potential for the ground state which comes from exchange interaction will be proportional to $\mathscr{J}(\mathbf{r})$ which adds a contribution to the central cell correction. This correction depends on a spin configuration of the composite system and is seen as different central cell correction for different levels. As long as the exchange interaction is small compared with localization energy, this correction is small compared with the main part and approach presented in this section may be used. Available experimental data show that it is the case of Mn acceptor. However, the effect of the exchange interaction for excited levels or for speculative magnetic impurity with similar exchange interaction and small binding energy demands for the exact solution.

VII. STM IMAGES

Observation of sub-surface neutral acceptor states by scanning tunneling microscopy[6,7,49,50] has been the origin of a considerable renewal of interest in acceptor physics.[33,35,47,51–53] In early papers,[7] the STM images were compared with cross sections of bulk impurity LDOS in a (110) plane. However, it appears that the situation is far more complex: indeed, in the vicinity of a (110) surface there is a large elastic deformation known as the "surface buckling".[54] Besides, the presence of the surface and the tip induced bend-bending add a perturbation qualitatively similar to the effect of an electric field acting on the hole. In addition, STM measures LDOS at some distance in the vacuum and this implies hybridization of impurity and dangling-bond states.[6] In Ref. 6, it was assumed that splitting by surface buckling (about 40 meV for an impurity in the fourth sublayer) was much larger than both thermal energy and exchange splitting. The magnetic interaction was therefore neglected, and it was assumed that only the ground state LDOS was observed in low temperature STM imaging. These conclusions were also supported by the fact that Zn and Cd acceptor in InP and GaAs,[8] which is non-magnetic, give images remarkably similar to Mn acceptor in GaAs. All thee impurities have very similar binding energy in the 100 meV range.

Complete discussion of STM results in the frame of present theory is beyond the scope of this paper, but we note that the analysis presented above suggests that for a strain induced splitting of 40 meV, exchange would be negligible for the $\epsilon = 5$ meV which is consistent with available experimental data.

VIII. CONCLUSION

We have re-examined the theory of neutral acceptor states within the *spds** extended-basis tight-binding model, that combines exact account of local symmetries and high accuracy of band dispersion representation. A spherical harmonic decomposition of the tight-binding LDOS has been used and allows both qualitative and quantitative analysis of the numerical results. The lifting of acceptor fourfold degeneracy by symmetry breaking perturbations like uniaxial strain or external electric field has been explicated, as well as the acceptor fine-structure arising from exchange interaction with d-electrons in the case of a magnetic impurity. This computational approach can be further improved by considering a full TB parameterization of the impurity central cell potential from comparisons with *ab initio* calculations of the "impurity material", as done in Ref. 6 for GaAs:Mn. The same formalism can provide realistic modeling of more complex situations like Mn-doped quantum dots, impurity pairing, sub-surface impurities and their STM imaging, or acceptor states in presence of external electric and magnetic fields.

Appendix A: Spherical harmonics

For completeness, we give a exact form of real spherical harmonics used in decomposition (3):

$$Y_{lm}(\Theta,\phi) = \begin{cases} \bar{P}_{lm}(\cos\Theta)\cos m\phi & \text{if } m \geq 0 \\ \bar{P}_{l|m|}(\cos\Theta)\sin|m|\phi & \text{if } m < 0 \end{cases}, \quad \text{(A1)}$$

where the normalized associated Legendre functions are given by

$$\bar{P}_{lm}(t) = \sqrt{(2-\delta_{0m})(2l+1)\frac{(l-m)!}{(l+m)!}}P_{lm}(t) \quad \text{(A2)}$$

with the following definition of the associated Legendre functions:

$$P_{lm}(t) = (1-t^2)^{m/2}\frac{d^m}{dt^m}P_l(t), \quad \text{(A3)}$$

$$P_l(t) = \frac{1}{2^l l!}\frac{d^l}{dt^l}(t^2-1)^l.$$

Appendix B: Spin operator in tight-binding

We follow philosophy of group representation theory, and start from the definition of state with angular momentum s as a wavefunction which transforms under action of space rotations under definite representation $\mathcal{D}_s^{\pm}$. Technically, this definition cannot be transferred to tight-binding directly, because tight-binding theory is not isotropic in accordance with space crystal symmetry. However, the same arguments apply for $\mathbf{k}\cdot\mathbf{p}$ model where

one still may work in the spherical approximation[2] and associate angular momentum with the states.

To generalize this approach to tight-binding we note that any point group is a subgroup of the full rotation group and thus its representations may be chosen as a subgroups of its representations as well. We choose basis function so that Γ_6, Γ_7 and Γ_8 are the subgroups of $\mathcal{D}^+_{1/2}$, $\mathcal{D}^-_{1/2}$, $\mathcal{D}^-_{3/2}$. Accordingly, we associate angular momentum with representations of T_d. This procedure should be used with care however, it only makes sense if one wants to discuss the results of the tight-binding in terms of $\mathbf{k}\cdot\mathbf{p}$ model or to transfer approximation used in $\mathbf{k}\cdot\mathbf{p}$ to TB and can not be extended beyond envelope function approach without additional assumptions.

As a result, we write spin operator as

$$\mathbf{J} = \sum_{i,\alpha} \alpha \left|\Gamma_{i,\alpha}\right\rangle \left\langle\Gamma_{i,\alpha}\right|, \tag{B1}$$

where i enumerates representations of T_d and $\alpha = \pm 1/2$ for $i = \Gamma_6, \Gamma_7$ and $\alpha = +3/2, +1/2, -1/2, -3/2$ for $i = \Gamma_8$. The functions $\left|\Gamma_{i,\alpha}\right\rangle$ are constructed from tight-binding orbitals. E.g., $\left|\Gamma_{6,+1/2}\right\rangle = |s\rangle\uparrow$, etc.

Approach (B1) might seem too formal at the first glance, however it provides two essential properties one usually expects from the theory: 1) it is very formal, contains no explicit assumptions on basis wavefunctions or any other details of the model and may be applied in any situation; 2) for the bulk states near band edges in unstrained zincblende semiconductor it gives results which are usually expected from the $\mathbf{k}\cdot\mathbf{p}$ theory, namely electron with spin 1/2 and holes with total spin 3/2 which are split to heavy and light holes with spin projection to momentum direction $\pm 3/2$ and $\pm 1/2$ respectively, etc.

ACKNOWLEDGMENTS

This work was supported by "Triangle de la Physique" (CAAS project), by International Ioffe Institute-CNRS Associate Laboratory ILNACS and by RFBR grants, and EU project SPANGL4Q

[1] J. M. Luttinger and W. Kohn, Phys. Rev. **97**, 869 (1955).
[2] A. Baldereschi and N. O. Lipari, Phys. Rev. B **8**, 2697 (1973).
[3] A. Baldereschi and N. O. Lipari, Phys. Rev. B **9**, 1525 (1974).
[4] T. G. Castner, Phys. Rev. B **77**, 205208 (2008).
[5] T. G. Castner, Phys. Rev. B **79**, 195207 (2009).
[6] J.-M. Jancu, J.-C. Girard, M. O. Nestoklon, A. Lemaître, F. Glas, Z. Z. Wang, and P. Voisin, Phys. Rev. Lett. **101**, 196801 (2008).
[7] A. M. Yakunin, A. Y. Silov, P. M. Koenraad, J. H. Wolter, W. Van Roy, J. De Boeck, J.-M. Tang, and M. E. Flatté, Phys. Rev. Lett. **92**, 216806 (2004).
[8] R. de Kort, M. C. M. M. van der Wielen, A. J. A. van Roij, W. Kets, and H. van Kempen, Phys. Rev. B **63**, 125336 (2001).
[9] E. L. Ivchenko, A. Y. Kaminski, and U. Rössler, Phys. Rev. B **54**, 5852 (1996).
[10] O. Krebs and P. Voisin, Phys. Rev. Lett. **77**, 1829 (1996).
[11] T. Ando and H. Akera, Phys. Rev. B **40**, 11619 (1989).
[12] Y. Fu, M. Willander, E. L. Ivchenko, and A. A. Kiselev, Phys. Rev. B **47**, 13498 (1993).
[13] T. B. Boykin, G. Klimeck, M. A. Eriksson, M. Friesen, S. N. Coppersmith, P. von Allmen, F. Oyafuso, and S. Lee, Applied Physics Letters **84**, 115 (2004).
[14] T. B. Boykin, G. Klimeck, M. Friesen, S. N. Coppersmith, P. von Allmen, F. Oyafuso, and S. Lee, Phys. Rev. B **70**, 165325 (2004).
[15] J.-M. Jancu, R. Scholz, G. C. La Rocca, E. A. de Andrada e Silva, and P. Voisin, Phys. Rev. B **70**, 121306 (2004).
[16] A. N. Poddubny, M. O. Nestoklon, and S. V. Goupalov, Phys. Rev. B **86**, 035324 (2012).
[17] M. O. Nestoklon, L. E. Golub, and E. L. Ivchenko, Phys. Rev. B **73**, 235334 (2006).
[18] M. O. Nestoklon, E. L. Ivchenko, J.-M. Jancu, and P. Voisin, Phys. Rev. B **77**, 155328 (2008).
[19] M. J. Schmidt, K. Pappert, C. Gould, G. Schmidt, R. Oppermann, and L. W. Molenkamp, Phys. Rev. B **76**, 035204 (2007).
[20] J. Bernholc and S. T. Pantelides, Phys. Rev. B **15**, 4935 (1977).
[21] N. Lipari, A. Baldereschi, and M. Thewalt, Solid State Communications **33**, 277 (1980).
[22] T. B. Boykin, L. J. Gamble, G. Klimeck, and R. C. Bowen, Phys. Rev. B **59**, 7301 (1999).
[23] T. B. Boykin, G. Klimeck, and F. Oyafuso, Phys. Rev. B **69**, 115201 (2004).
[24] J.-M. Jancu, R. Scholz, F. Beltram, and F. Bassani, Phys. Rev. B **57**, 6493 (1998).
[25] J.-M. Jancu and P. Voisin, Phys. Rev. B **76**, 115202 (2007).
[26] Y. M. Niquet, D. Rideau, C. Tavernier, H. Jaouen, and X. Blase, Phys. Rev. B **79**, 245201 (2009).
[27] M. Zieliński, Phys. Rev. B **86**, 115424 (2012).
[28] A. K. Bhattacharjee and C. B. à la Guillaume, Solid State Commun. **113**, 17 (2000).
[29] G. F. Koster, J. O. Dimmock, R. G. Wheeler, and H. Statz, The Properties of the Thirty-Two Point Groups (M.I.T. Press, Cambridge, 1963).
[30] G. L. Bir, E. I. Butikov, and G. E. Pikus, J. Phys. Chem. Solids **24**, 1467 (1963).
[31] W. Schairer and M. Schmidt, Phys. Rev. B **10**, 2501 (1974).
[32] T. N. Morgan, Phys. Rev. B **12**, 5714 (1975).
[33] C. Bihler, G. Ciatto, H. Huebl, G. Martinez-Criado, P. J. Klar, K. Volz, W. Stolz, W. Schoch, W. Limmer, F. Filippone, A. Amore Bonapasta, and M. S. Brandt, Phys. Rev. B **78**, 235208 (2008).
[34] J. Schneider, U. Kaufmann, W. Wilkening, M. Baeumler, and F. Köhl, Phys. Rev. Lett. **59**, 240 (1987).

[35] G. V. Astakhov, R. I. Dzhioev, K. V. Kavokin, V. L. Korenev, M. V. Lazarev, M. N. Tkachuk, Y. G. Kusrayev, T. Kiessling, W. Ossau, and L. W. Molenkamp, Phys. Rev. Lett. **101**, 076602 (2008).

[36] A. Kudelski, A. Lemaître, A. Miard, P. Voisin, T. C. M. Graham, R. J. Warburton, and O. Krebs, Phys. Rev. Lett. **99**, 247209 (2007).

[37] O. Krebs, E. Benjamin, and A. Lemaître, Phys. Rev. B **80**, 165315 (2009).

[38] O. Krebs and A. Lemaître, Phys. Rev. Lett. **111**, 187401 (2013).

[39] M. Linnarsson, E. Janzén, B. Monemar, M. Kleverman, and A. Thilderkvist, Phys. Rev. B **55**, 6938 (1997).

[40] N. Averkiev, A. Gutkin, and E. Osipov, Sov. Phys. Semicond. **21**, 1119 (1987).

[41] e. a. N.S. Averkiev, Fiz. Tverd. Tela **30**, 765 (1988), sov. Phys. Solid State 30 (1988) 438.

[42] V. Sapega, T. Ruf, and M. Cardona, Solid State Commun. **114**, 573 (2000).

[43] V. F. Sapega, T. Ruf, and M. Cardona, Phys. Stat. Solidi (b) **226**, 339 (2001).

[44] V. F. Sapega, M. Moreno, M. Ramsteiner, L. Däweritz, and K. Ploog, Phys. Rev. B **66**, 075217 (2002).

[45] D. A. Varshalovich, A. N. Moskalev, and V. K. Khersonskii, Quantum theory of angular momentum (World Scientific, 1988).

[46] We again remind that in tight-binding approximation this level has Γ_8 symmetry and not $D_{3/2}$.

[47] T. O. Strandberg, C. M. Canali, and A. H. MacDonald, Phys. Rev. B **80**, 024425 (2009).

[48] M. O. Nestoklon, O. Krebs, H. Jaffrs, S. Ruttala, J.-M. George, J.-M. Jancu, and P. Voisin, Applied Physics Letters **100**, 062403 (2012).

[49] G. Mahieu, B. Grandidier, D. Deresmes, J. P. Nys, D. Stiévenard, and P. Ebert, Phys. Rev. Lett. **94**, 026407 (2005).

[50] S. Loth, M. Wenderoth, L. Winking, R. G. Ulbrich, S. Malzer, and G. H. Döhler, Phys. Rev. Lett. **96**, 066403 (2006).

[51] J.-M. Tang and M. E. Flatté, Phys. Rev. B **72**, 161315 (2005).

[52] C. Çelebi, J. K. Garleff, A. Y. Silov, A. M. Yakunin, P. M. Koenraad, W. Van Roy, J.-M. Tang, and M. E. Flatté, Phys. Rev. Lett. **104**, 086404 (2010).

[53] A. Richardella, D. Kitchen, and A. Yazdani, Phys. Rev. B **80**, 045318 (2009).

[54] B. Engels, P. Richard, K. Schroeder, S. Blügel, P. Ebert, and K. Urban, Phys. Rev. B **58**, 7799 (1998).